Self-consistent semirelativistic energy bands of WSi_2

Bijan K. Bhattacharyya, D. M. Bylander, and Leonard Kleinman
Department of Physics, University of Texas, Austin, Texas 78712
(Received 20 August 1984)

The WSi_2 energy bands, projected densities of states, and cohesive energy have been calculated self-consistently with use of the semirelativistic pseudopotential for the experimental equilibrium lattice as a function of the W—Si bond length. The cohesive energy and W—Si bond length are in good agreement with experiment. Additionally, we obtain the symmetric phonon frequency.

I. INTRODUCTION

Transition-metal—semiconductor contacts are widely used in the semiconductor industry because of their stability and reliability. The refractory-metal silicides WSi_2 and $MoSi_2$, which along with $ReSi_2$ crystallize in the body-centered tetragonal CaC_2 structure, are very promising as materials for improved gate electrodes and interconnection lines in very-large-scale integrated circuits. These materials are more conductive (by at least an order of magnitude) than the presently used heavily doped polycrystalline silicon and are much more oxidation resistant than pure metals. As far as we know there have been no energy-band calculations of these crystals heretofore. In this paper we calculate the energy bands, projected densities of states and cohesive energy of WSi_2 self-consistently using our semirelativistic pseudopotential[1,2] which includes all relativistic effects except spin orbit to order α^2, where α is the fine-structure constant.

The body-centered tetragonal unit cell of WSi_2 is shown in Fig. 1. We performed the calculations with the lattice constants quoted by Goldschmidt,[3] $c=7.868$ Å and $a=3.211$ Å which differ slightly from those of Wyckoff,[4] $c=7.880$ Å and $a=3.212$ Å. Although Wyckoff gives the W—Si bond length, $u=0.33c$, in an earlier edition,[5] he does not quote a value for it in his most recent work[4] and we take it as a variable whose equilibrium value maximizes the cohesive energy. This also allows us to calculate the symmetric optical-phonon frequency.

The Brillouin zone (BZ) is displayed in Fig. 2 with symmetry points and lines labeled with a standard notation.[6(a)] In addition we have labeled points a, b, c, and d which have no extra symmetry but which lie at the ends of lines along which we have calculated the energy bands. For $c>\sqrt{3}a$ the primitive reciprocal lattice vectors are $\mathbf{K}_1=(0,0,4\pi/c)$, $\mathbf{K}_2=(2\pi/a,0,2,\pi/c)$, and $\mathbf{K}_3=(0,2\pi/a,2\pi/c)$. To increase the confusion, many references[6(b)] rotate the BZ coordinates by 45° so that $\mathbf{K}_2'=(2\pi/a',2\pi/a',2\pi/c)$ and $\mathbf{K}_3'=(2\pi/a',-2\pi/a',2\pi/c)$ with $a'=\sqrt{2}a$. When $c=a'=\sqrt{2}a$ the body-centered tetrahedral lattice becomes an fcc lattice and this makes the reciprocal lattice vectors explicitly identical but it

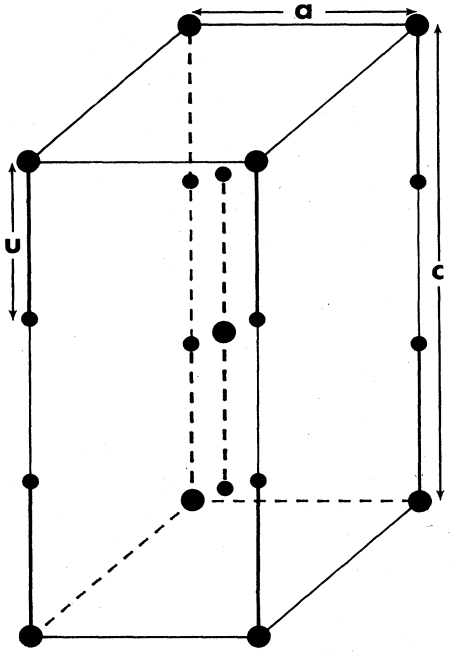

FIG. 1. Body-centered tetragonal unit cell of WSi_2 with large circles representing W and small circles representing Si.

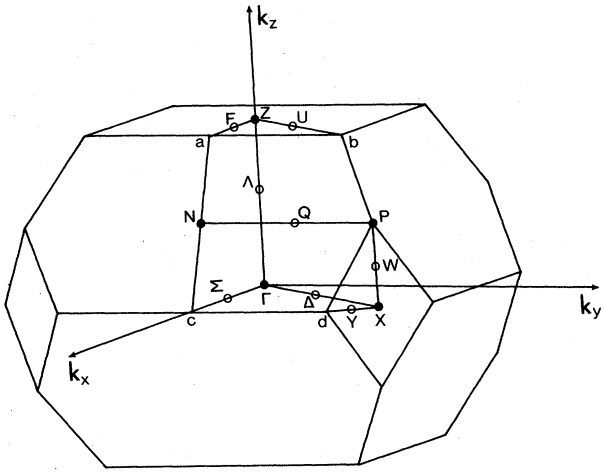

FIG. 2. Body-centered tetragonal Brillouin zone for $c>a$. The points a, b, c, and d are not symmetry points but are labeled to facilitate comparison with the energy bands of Fig. 3.

seems to us to be an unnatural choice when the crystal is not cubic.

In the next section, we briefly describe our computational method which differs in several details from our semirelativistic W calculation.[7] In Sec. III our results are presented.

II. COMPUTATIONAL METHOD

We expand our wave function in a total of 88 basis functions consisting of three Gaussians times each s, p, and d spherical harmonic on each of the three atoms in the unit cell plus a single Gaussian times each of the f spherical harmonics on the W atom. The shortest-range W d Gaussian was contracted with an even shorter-range Gaussian. The Gaussian exponents and contraction ratio were determined by trail and error for each calculation with different u by minimizing the lowest eigenvalues with various symmetries at Γ. The eigenvalues are most sensitive to the W d—Gaussian exponents; an estimate of the convergence error inherent in our basis set may be gleaned from the fact that an additional 16-meV convergence was obtained for Γ_3^+, a pure d state, when seven W and four Si d Gaussians were used.

The calculations were iterated to self-consistency by sampling 784 points in a primitive cell (not the BZ) in reciprocal space. This cell is $\sqrt{2}(2\pi/a)\times\sqrt{2}(2\pi/a)\times(2\pi/c)$ and we chose the points $(\pm n/28)[\sqrt{2}[(2\pi/a)]],(\pm m/28)[\sqrt{2}(2\pi/a)]],(\pm p/8)(2\pi/c)$, with m and n all odd integers <14 and p all odd integers <4. These 784 points reduce to 56 in the $\frac{1}{16}$th irreducible wedge of this cell. Note that because the ratio $(28a/\sqrt{2})/8c = 1.010$, this array is almost perfectly cubic.

Because of the larger unit cell here we were not able to calculate Fourier components of the charge density ρ from the wave functions as we did for W. Rather, we calculated ρ at 1220 points selected randomly throughout the unit cell plus 127 points selected at random angles on radial meshes centered on the three atoms in the cell for a total of 1600 independent points.[8] Each of these points (except for those at the origin of a radial mesh) are, by symmetry, equivalent to 16 points in the unit cell. We put a Gaussian charge on each atom to screen the Z/r tail of the pseudopotential and then fit the crystal charge with those Gaussians plus 143 functions which did not contain any net charge and whose coefficients were varied to minimize the rms error at the 1600 points. These fitting functions consist of the first 59 symmetrized combination of plane waves (SCPW), excluding the zeroth, plus functions of the form[9] $\nabla^2[K_{lm}(\theta,\phi)e^{-\alpha r^2}]$, where K_{lm} is a combination of spherical harmonics with the crystal symmetry on an atomic site of which there are one s, one d, and two g on W and one s, p, d, and f and two g on Si. For each of these K_{lm} we used 8 different Gaussians except for the s for which we used ten. To test the accuracy of the fit we let the coefficients of the Gaussian screening charges be variables and obtained $Z_W+2Z_{Si}=13.9998$. The exchange-correlation potential was calculated at the same 1600 points and fit with the same set of $K_{lm}(\theta,\phi)e^{-\alpha r^2}$ plus the first 80 SCPW, including the zeroth.

We used the same Wigner correlation and relativistic Kohn-Sham exchange potentials as in Ref. 7. We defined $V_{xc}^{val}(\mathbf{r})$ to be $V_{xc}(\rho_T(\mathbf{r}))-V_{xc}(\rho_c(r))$, where ρ_T and ρ_c are total and core ρ's but since we are using a rigid core, the calculation is independent[10] of $V_{xc}(\rho_c(r))$; thus for computational ease we cut off the long-range tail of $V_{xc}(\rho_c(r))$ without introducing any error. The W semirelativistic pseudopotential[1,2] is identical to that of Ref. 7 except that we fit the local part of the pseudopotential V_L plus the screening Gaussian charge potential with a set of spherical Gaussians. The small difference between the actual potential and the fit was then included in the nonlocal part of the pseudopotential, V_{NL}. This enabled us to calculate the three-center matrix elements of V_L analytically while performing the two-center V_{NL} matrix element integrations numerically. The Si pseudopotential was constructed in exactly the same manner except that $l_{max}=2$ rather than 3.

The binding energy is calculated variationally,[11]

$$-E_{binding}=\sum_{n,\mathbf{k}}\epsilon_{n,\mathbf{k}}-\sum_{\mathbf{K}}V(\mathbf{K})\rho(\mathbf{K})+\tfrac{1}{2}4\pi\Omega\sum_{\mathbf{K}}{}'\rho^2(\mathbf{K})/K^2+\int_\Omega d^3r[\epsilon_{xc}(\rho_T)\rho_T-\epsilon_{xc}(\rho_c)\rho_c]+E_{Ewald}\,.$$

Here $V(\mathbf{K})=V_{Coul}^{val}(\mathbf{K})+V_{xc}^{T}(\mathbf{K})$ is an input potential

TABLE I. Contributions to the cohesive energy of WSi_2 for three different values of the W—Si bond length u. All energies are in hartrees except for the cohesive energy which is in eV.

u	$0.327c$	$0.337c$	$0.345c$
$\sum_{n,\mathbf{k}}\epsilon_{n,\mathbf{k}}$	0.818 633	0.949 486	1.015 223
$-\sum_{\mathbf{K}}V(\mathbf{K})\rho(\mathbf{K})$	10.275 058	10.080 226	9.909 899
$\frac{1}{2}(4\pi\Omega)\sum_{\mathbf{K}}{}'\rho^2(\mathbf{K})/K^2$	0.172 871	0.204 111	0.252 775
$\int[\epsilon_{xc}(\rho_T)\rho_T-\epsilon_{xc}(\rho_c)\rho_c]$	−5.911 902	−5.919 750	−5.930 627
E_{Ewald}	−21.376 356	−21.340 383	−21.269 854
$-E_{binding}$	−16.021 696	−16.026 310	−16.022 584
E_{atom}	15.279 284	15.279 284	15.279 284
$E_{cohesive}$	20.2010 eV	20.3266 eV	20.2252 eV

TABLE II. Calculated cohesive energy after each iteration. The second column is a measure of how far the potential is from self-consistency.

Iteration	$\delta(\Delta(r))$ (eV)	E_{cohesive} (eV)
0	3.03	20.188 75
1	1.40	20.311 90
2	0.30	20.325 42
3	0.14	20.326 37
4	0.045	20.326 56
5	0.030	20.326 59
6	0.011	20.326 54
7	0.006	20.326 62
8	0.003	20.326 59

which results in an output valence charge density $\rho(\mathbf{K})$ and $V_{\text{xc}}^{T}(\mathbf{K})$ is a Fourier transform of $V_{\text{xc}}(\rho_T(\mathbf{r}))$. The exchange functional in the fourth term was fit in the same way as $V_{\text{xc}}^{\text{val}}(\mathbf{r})$ and integrated analytically except that the number of s fitting functions was increased from 10 to 24 and SCPW from 80 to 100. Although there is a certain amount of arbitrariness in $\epsilon_{\text{xc}}(\rho_c)\rho_c$, the same quantity is subtracted from the atomic energy and therefore it cancels from the cohesive energy. The first term, the sum of the one-electron energies, minus the second, is equal to the kinetic energy plus pseudopotential energy of the valence electrons. Note that the zero of Coulomb potential which is an arbitrary quantity (whose value is dependent on the choice of fitting functions[12]) cancels out of the first two terms. The third term represents the valence electron self-Coulomb interaction, excluding the zeroth Fourier component of the valence charge density, which when combined with the ionic point charges Z_{W} and the two Z_{Si} yields the last term, E_{Ewald}. The formula for E_{Ewald} depends on the W—Si bond length u and was calculated in the manner first described by Fuchs.[13].

In Ref. 7 we subtracted $\frac{1}{2}(4\pi\Omega)\sum_{\mathbf{K}}'\rho^2(\mathbf{K})/K^2$ rather than adding it and subtracting $\sum_{\mathbf{K}} V_{\text{Coul}}^{\text{val}}(\mathbf{K})\rho(\mathbf{K})$. The two are equivalent when the calculation has converged so that $V_{\text{Coul}}^{\text{val}}(\mathbf{K})=4\pi\rho(\mathbf{K})/K^2$ is unchanged by further iteration.

III. RESULTS

In Table I we display all the contributions to E_{binding} for three different values of the W—Si bond length u. The atomic energies were calculated with the relativistic spin-polarized[14,15] Kohn-Sham-Wigner exchange-correlation energy functional and the semirelativistic pseudopotential. They are $E_{\text{W}}=15.312\,349$ Ry and $E_{\text{Si}}=7.623\,109$ Ry. $E_{\text{atom}}=E_{\text{W}}+2E_{\text{Si}}$ is listed in the next to last row of Table I and subtracted from E_{binding} to yield the cohesive energy in the last row. Fitting the cohesive energy with a parabola yields $u_0=2.6465$ Å $=0.3364c$ and $E_{\text{cohesive}}^{\text{max}}=20.3270$ eV. The zero-point vibrational energy should reduce $E_{\text{cohesive}}^{\text{max}}$ by about 0.1 eV. The value of u_0 is very close to the $0.33c$ quoted by Wyckoff.[5] We compare $E_{\text{cohesive}}^{\text{max}}$ with the experimental value $E_{\text{cohesive}}^{\text{exp}}=E_{\text{W}}+2E_{\text{Si}}+H=8.90+9.26+0.97=19.13$ eV where E_{W} and E_{Si} are the experimental cohesive energies[16] of W and Si and $-H$ is the heat of for-

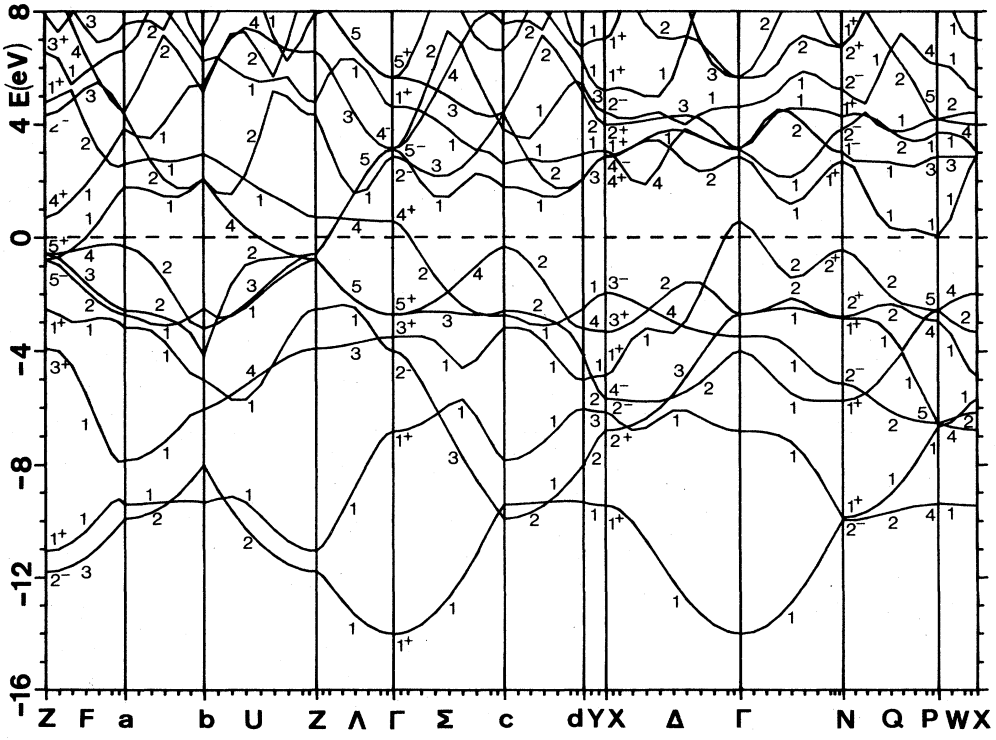

FIG. 3. The energy bands of WSi_2 for $u=0.337c$ calculated along lines in the BZ shown in Fig. 2. Eigenvalues were calculated at each tic mark along the abscissa. The energy is measured from E_F.

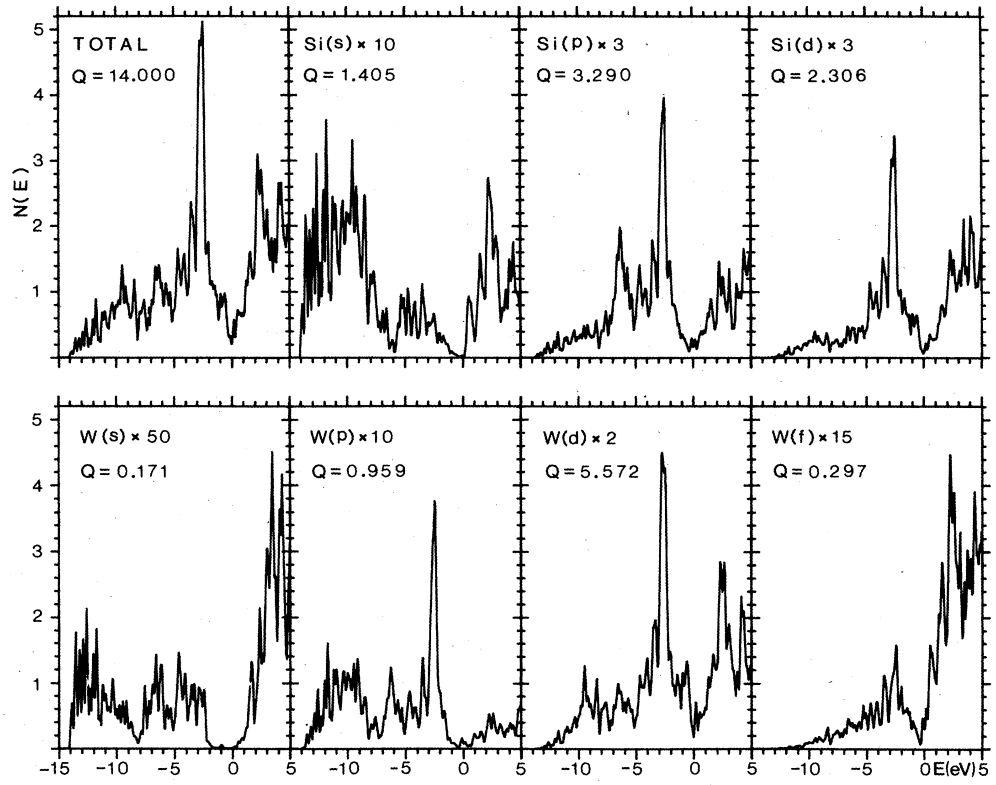

FIG. 4. Total density of states and projected DOS of WSi_2 for $u=0.337c$ in units of electrons per eV per unit cell. Q is the total charge of each type integrated up to E_F, where $E=0$ is E_F.

mation[3] of WSi_2. This discrepancy, with the calculated cohesive energy several percent larger than the experimental, is typical of numerically accurate calculations made with a local density approximation for exchange and correlation. Our parabolic fit yields $-E_{\text{cohesive}} = -E^{\max}_{\text{cohesive}} + \frac{1}{2}k(u-u_0)^2$ with $(u-u_0)$ in cm and $k=7.248\times10^5$ dyn/cm. This yields[17] a frequency for the symmetric optical phonon, $\nu=14.00\times10^{12}$ Hz. We could not find an experimental value for this phonon frequency but, for comparison, the optical frequency of elemental Si is[18] 15.25×10^{12} Hz.

Chelikowski and Louie[11] have claimed that, if the cohesive energy is calculated variationally, a non-self-consistent potential, obtained from a superposition of atomic charge densities, yields a value acceptably close to that obtained from the self-consistent potential. We see from Table II where we list the cohesive energy obtained after each iteration for $u=0.337c$, that their claim is substantiated. Because the zero of potential is arbitrary, $\Delta(\mathbf{r})=V_{\text{input}}(\mathbf{r})-V_{\text{output}}(\mathbf{r})$ is not a measure of how far the calculation is from convergence but the difference between the maximum and minimum values of $\Delta(\mathbf{r})$ is. This is listed in the second column of Table II. Thus we see, after no iterations the potential is unconverged by 3 eV, but E_{cohesive} is within 0.18 eV of its converged value. After just two iterations when the potential still is 0.30 eV from convergence, E_{cohesive} has converged to within 0.001 eV. After convergence, random noise of ±0.00004 eV occurs in E_{cohesive}. This is a measure of the random error introduced by fitting the potential.

In Fig. 3 we show the energy bands for $u=0.337c$ calculated along eleven different lines in the BZ. Those lines with no symmetry beyond that of the plane in which they lie are unlabeled. Figure 4 displays the density of states together with Löwden projections[19] of the density of states (DOS) onto the orbital symmetries in our basis set. The dip which is present in the DOS at the Fermi energy also occurs for $NiSi_2$,[20,21] $CoSi_2$,[21] and Ni_3Si.[22] The total charge density due to orbitals of each symmetry, obtained by integrating the projected DOS up to E_F is given in the figure. Adding up the projected charges on each atom we find 6.999 electrons on the W and 7.001 on both Si; thus the Si ionicity is $+0.50$ and the W ionicity is -1.00. This can be compared with the ionicities we calculated[20] for $NiSi_2$: -1.12 for Ni and $+0.56$ for Si. It should be pointed out, however, that the ionicity is a very strong function of exactly how it is defined. The ionicity of $NiSi_2$ was very small when it was obtained by comparing the charge in a 1-Å radius sphere about an Si atom in $NiSi_2$ with that in the same size sphere about an atom in a silicon crystal.[21] In Table III we list Löwdin projected symmetry content of individual eigenstates at the Γ, Z, X, and N points of the BZ. From both Table III and Fig. 4 we see that although the bottom of the bands is almost pure s, the total s contribution to the occupied bands is small, and to the 5 eV below E_F is almost negligible.

TABLE III. Löwdin projection (%) of the symmetry content of all the states at the symmetry points Γ, Z, X, and N shown in Fig. 3.

E (eV)		W(s)	W(p)	W(d)	W(f)	Si(s)	Si(p)	Si(d)
Γ_1^+	−14.0166	14.76	0	0.19	0	85.01	0.01	0.03
Γ_1^+	−6.8238	1.13	0	59.39	0	0.07	33.04	6.37
Γ_2^-	−4.0156	0	13.59	0	14.82	39.25	6.27	26.07
Γ_3^+	−3.4976	0	0	82.57	0	0	0	17.43
Γ_5^+	−2.7167	0	0	56.79	0	0	37.64	5.57
Γ_4^+	0.5627	0	0	86.88	0	0	0	13.12
Γ_2^-	2.8538	0	9.14	0	14.90	27.90	22.32	25.74
Γ_5^-	3.1143	0	11.45	0	20.14	0	42.57	25.84
Γ_4^-	3.1403	0	0	0	15.57	0	0	84.43
Γ_1^+	4.6109	3.58	0	70.26	0	0.63	13.97	11.56
Γ_5^+	5.6533	0	0	54.22	0	0	32.36	13.42
Z_2^-	−11.8000	0	31.08	0	0.06	48.66	10.05	10.15
Z_1^+	−11.0716	9.43	0	39.29	0	23.31	26.87	1.10
Z_3^+	−3.9260	0	0	77.78	0	0	0	22.22
Z_1^+	−2.5213	2.99	0	47.27	0	0.96	9.80	38.98
Z_5^-	−0.7732	0	13.35	0	15.70	0	68.62	2.33
Z_5^+	−0.5690	0	0	76.91	0	0	9.77	13.32
Z_4^+	0.7083	0	0	88.04	0	0	0	11.96
Z_2^-	4.3197	0	1.46	0	37.03	3.82	56.38	1.31
Z_1^+	4.7695	7.79	0	17.91	0	56.69	17.33	0.28
Z_3^+	6.5577	0	0	27.17	0	0	0	72.83
Z_1^+	7.9151	8.32	0	15.54	0	0.05	33.21	42.88
N_2^-	−9.9938	0	29.81	0	2.27	40.88	9.20	17.84
N_1^+	−9.8774	3.25	0	54.13	0	16.83	22.66	3.13
N_1^+	−5.7510	2.92	0	50.97	0	4.90	15.06	26.15
N_2^-	−5.1555	0	25.20	0	5.88	0.38	66.57	1.97
N_1^+	−2.8446	0.42	0	66.32	0	0.02	13.93	19.31
N_2^+	−2.8037	0	0	60.32	0	0	25.20	14.48
N_2^+	−0.4332	0	0	71.90	0	0	0.21	27.89
N_1^+	2.6726	3.42	0	89.03	0	0.05	6.35	1.15
N_1^-	3.0010	0	0.80	0	20.25	0	54.12	24.83
N_2^-	3.8042	0	3.60	0	28.59	8.04	40.05	19.72
N_1^+	4.2909	4.11	0	66.43	0	18.62	2.10	8.74
N_2^-	5.2372	0	9.23	0	22.32	7.09	4.01	57.35
N_2^+	6.7326	0	0	37.85	0	0	45.99	16.16
N_1^+	6.7769	8.91	0	3.90	0	16.68	19.63	50.88
X_1^+	−9.4710	0.03	0	68.21	0	19.27	3.13	9.36
X_2^+	−6.7959	0	0	57.80	0	0	36.54	5.66
X_2^-	−6.1637	0	28.63	0	2.86	0	65.74	2.77
X_4^-	−5.6823	0	4.97	0	15.70	46.47	5.25	27.61
X_1^+	−4.8731	1.64	0	36.46	0	2.93	30.50	28.47
X_3^+	−3.3337	0	0	64.82	0	0	16.86	18.32
X_3^-	−1.9659	0	27.93	0	1.42	0	30.41	40.24
X_4^+	2.8485	0	0	99.85	0	0	0	0.15
X_4^-	2.8844	0	7.80	0	23.15	10.99	31.84	26.22
X_1^+	3.0598	3.01	0	77.43	0	4.60	1.52	13.44
X_2^+	3.9961	0	0	63.50	0	0	8.45	28.05
X_2^-	4.4344	0	15.28	0	15.59	0	0.30	68.83
X_1^+	5.1987	21.61	0	40.28	0	18.92	0.83	18.36
X_1^+	7.0304	11.19	0	38.50	0	0.61	26.38	23.32

Figures 5 and 6 are contours of constant pseudocharge density in (100) and (110) planes. Note that each W has eight nearest-neighbor Si arranged in square arrays above and below it and two second-neighbor Si directly above and below it. Similarly, each Si has four nearest-neighbor W in a square array either above or below it and one second neighbor either directly below or above it. For $u = 0.337c$, the first two W—Si bond lengths are almost

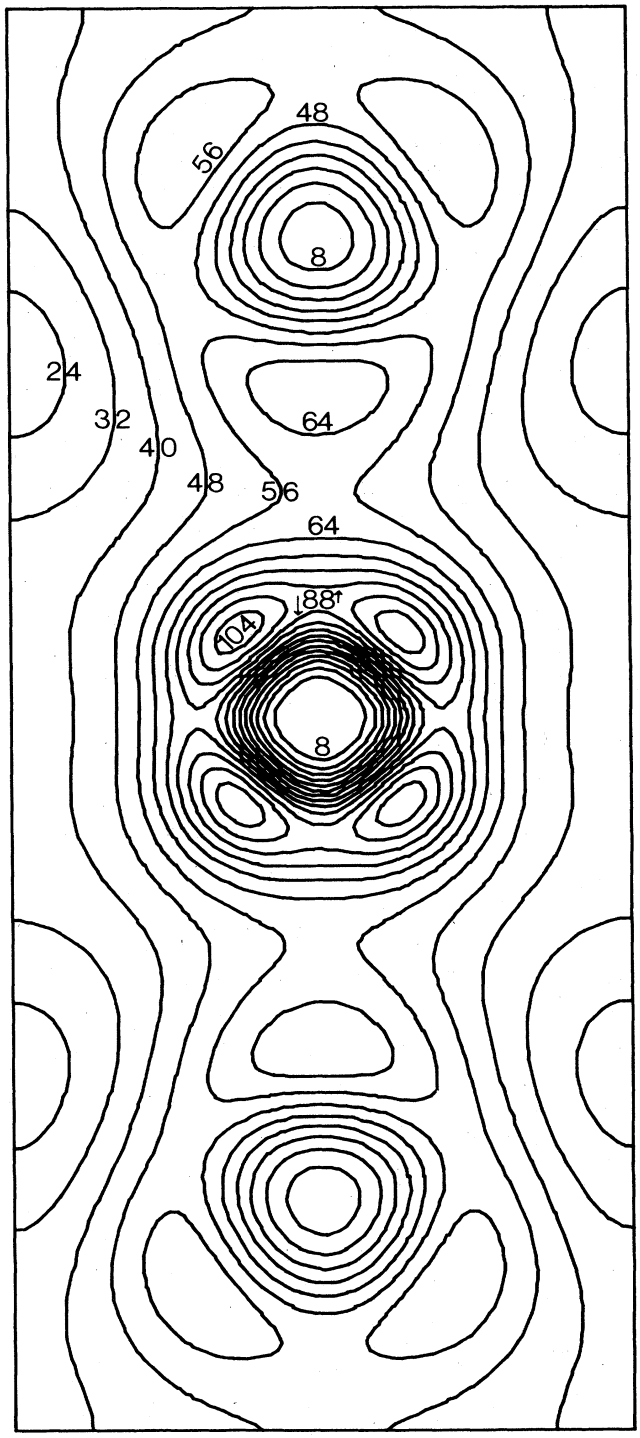

FIG. 5. Contours of constant pseudocharge density in a (100) plane in steps of 8 millielectrons per cubic bohr.

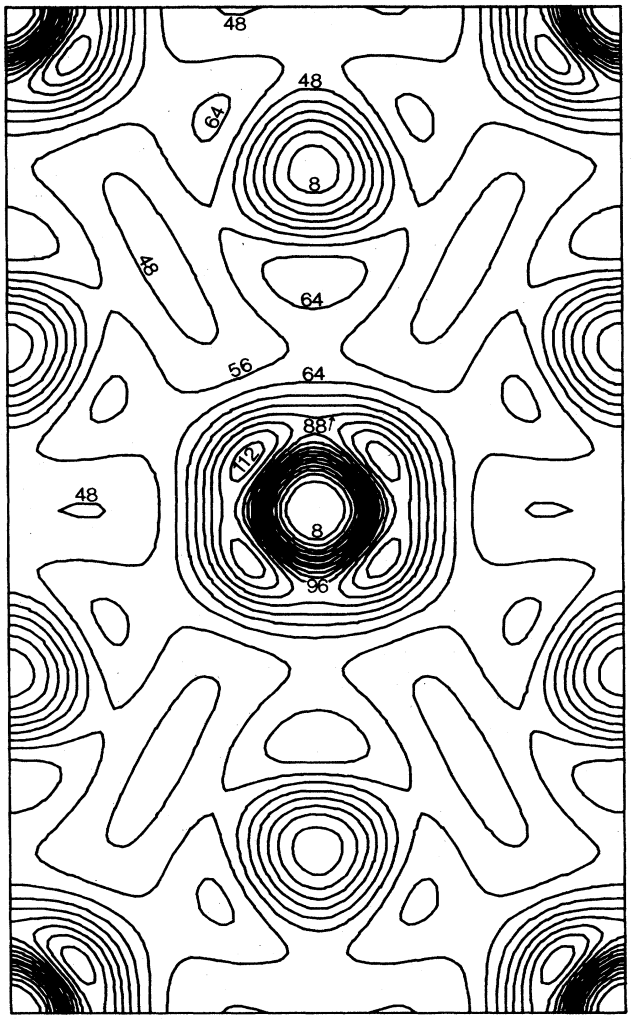

FIG. 6. Contours of constant pseudocharge density in a (110) plane in steps of 8 millielectrons per cubic bohr.

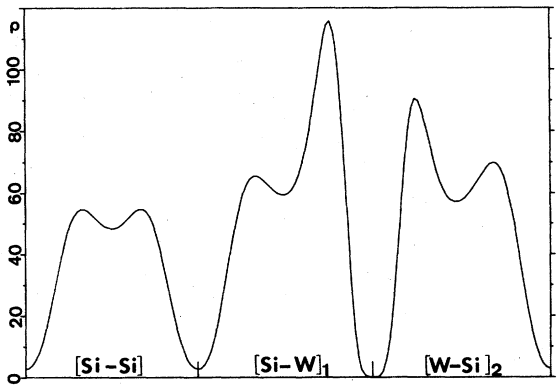

FIG. 7. Plot of pseudocharge density along Si—Si nearest-neighbor bond and Si—W first- and second-nearest-neighbor bonds in units of millielectrons per cubic bohr.

identical: 2.608 and 2.652 Å. Each Si has one Si nearest neighbor 2.565 Å directly above or below it and four second neighbors in a square array either below or above it 3.025 Å away. In Fig. 7 we plot the charge density

along the Si—Si first neighbor direction and the first and second Si—W neighbor directions. We see that each covalent bond is doubly peaked with the W peak in the W—Si first-neighbor bond much larger than in the second-neighbor bond with the Si peak somewhat larger in the second-neighbor bond than in the first. It is this covalent bonding which causes the dip in the DOS at the Fermi energy. Thus as with the other silicides we have examined,[20,22] we find that the binding energy has metallic, ionic, and covalent components.

ACKNOWLEDGMENTS

This work was supported by the Robert A. Welch Foundation (Houston, Texas) and by the National Science Foundation under Grant No. DMR-80-19518.

[1]L. Kleinman, Phys. Rev. B **21**, 2630 (1980).

[2]L. Kleinman and D. M. Bylander, Phys. Rev. Lett. **48**, 1425 (1982).

[3]H. J. Goldschmidt, *Interstitial Compounds* (Plenum, New York, 1967).

[4]R. W. G. Wyckoff, *Crystal Structures,* 2nd ed. (Interscience, New York, 1963), Vol. 1.

[5]R. W. G. Wyckoff, *The Structure of Crystals* (Chemical Catalog, New York, 1931).

[6](a) C. J. Bradley and A. P. Cracknell, *The Mathematical Theory of Symmetry in Solids* (Clarendon, Oxford, 1972), p. 105; (b) See, for example, M. Lax, *Symmetry Principles in Solid States and Molecular Physics* (Wiley, New York, 174), p. 449.

[7]D. M. Bylander and L. Kleinman, Phys. Rev. B **27**, 3152 (1983).

[8]Since the origins of the two Si meshes are equivalent by symmetry, we only included one of them.

[9]Note that this directly yields a Coulomb potential of the form $K_{lm}(\theta,\phi)e^{-\alpha r^2}$.

[10]The atomic V_{xc}^{val} is subtracted from the atomic pseudopotential to form the ionic pseudopotential; since the same $V_{xc}(\rho_c)$ is subtracted from the atomic V_{xc}^{val} as from the crystal V_{xc}^{val}, it does not in fact enter the calculation at all.

[11]J. R. Chelikowsky and S. G. Louie, Phys. Rev. B **29**, 3470 (1984).

[12]Its value is equal to the sum of the zeroth Fourier transform of the various $K_0(\theta,\phi)e^{-\alpha r^2}$ times their coefficients plus the sum of the zeroth Fourier transforms of the potential due to point charges, Z_W plus two Z_{Si}, with their screening Gaussian charges.

[13]K. Fuchs, Proc. R. Soc. London Ser. A **151**, 585 (1935).

[14]U. von Barth and L. Hedin, J. Phys. C **5**, 1629 (1972).

[15]D. M. Bylander and L. Kleinman, Phys. Rev. Lett. **51**, 889 (1983), see Ref. 11 therein.

[16]C. Kittel, *Introduction to Solid State Physics,* 5th ed. (Wiley, New York, 1976), p. 74.

[17]This is most easily obtained by noting that the W atom is stationary in this mode so that it is equivalent to each Si vibrating with half the energy against an infinitely massive object. Thus $E'=\frac{1}{2}k'(u-u_0)^2$ with $E'=\frac{1}{2}E$ and $k'=\frac{1}{2}k$ so that $\nu=(1/2\pi)\sqrt{k'/M_{Si}}$.

[18]B. N. Brockhouse, Phys. Rev. Lett. **2**, 256 (1959).

[19]P. O. Löwdin, J. Chem. Phys. **18**, 365 (1950).

[20]D. M. Bylander, L. Kleinman, K. Mednick, and W. R. Grise, Phys. Rev. B **26**, 6379 (1982). Note that ionicities in Ref. 20 were defined with a sign convention opposite to the standard convention used in this paper.

[21]J. Tersoff and D. R. Hamann, Phys. Rev. B **28**, 1168 (1983).

[22]D. M. Bylander, L. Kleinman, and K. Mednick, Phys. Rev. B **25**, 1090 (1982).